

# Regional Stabilizing and $H_2$ Control with Actuator Saturation using Linear Matrix Inequalities

Yeong-Hwa Chang\*, Yuan-Yuan Wang\*\*, Min-Hsiung Hung\*\*  
and Pang-Chia Chen\*\*\*

\*Department of Electrical Engineering, Chang Gung University (Corresponding Author)

\*\*Department of Electrical Engineering, Chung Cheng Institute of Technology, National Defense University

\*\*\*Department of Aircraft Engineering, the Air Force Institute of Technology

## ABSTRACT

In this paper, a linear system with actuator saturation is addressed. Based on certain LMI formulations, regional stabilizing is achieved along with  $H_2$  performance. A certain stripe in the open left half plane is the pole placement region of interest. Sufficient conditions to ensure the regional stability are derived. The  $H_2$  suboptimal control is also investigated, where the  $H_2$  performance index is within a designed value by utilizing state feedback control scheme. Examples are provided to illustrate the feasibility of the proposed work.

**Keywords:** Actuator saturation, LMI, Regional stability,  $H_2$  control

## 線性矩陣不等式為基礎之致動器飽和系統區域穩定與 $H_2$ 控制

張永華\* 王元元\*\* 洪敏雄\*\* 陳邦家\*\*\*

\*長庚大學電機系      \*\*國防大學中正理工學院電機系

\*\*\*空軍航空技術學院飛機系

## 摘 要

本文旨在以線性矩陣不等式為基礎，探討系統具致動器飽和限制之區域穩定與  $H_2$  控制。在狀態回授控制架構下，將推導出滿足系統特性根限制在左半平面的帶狀區域內之穩定條件，同時相關的  $H_2$  性能指標亦可符合預先設定值。不同的例子將用來說明本文所提方法的可行性。

**關鍵字：**致動器飽和、線性矩陣不等式、區域穩定、 $H_2$  控制

## I. INTRODUCTION

Practically, in order to avoid possible damage of actuator, the performance limitations of actuator must be considered. Usually, a certain chop scenario according to the maximum allowable signal amplitude is applied to protect overload operations. In common, a saturation device is added in front of the controlled plant to model a input-constrained control system. However, with the consideration of saturation, the related analysis and synthesis issues become more complex and even more the resulted system may become unstable.

The topics of constrains have been attracted a lot of attention [1]. In general, we can manipulate a saturation device as the assembly of linear and nonlinear items. With the standpoint of robustness, the nonlinear item can be considered as an exogenous disturbance. Ideally, if these virtual disturbances can be controlled and limited in a range of bound, the stability of control system will be achieved. Versatile methods and applications of constrained systems have been discussed and implemented in recent years. Saberi et. al. employed feedback laws with low-and-high gain structure to solve several semiglobal control problems for asymptotically null controllable linear systems with bounded controls where the input is subject to magnitude saturation [2]. It is shown that robust semiglobal disturbance rejection can be achieved with linear state feedback. Moreover, with a minimum phase and left invertibility assumption, similar results can be achieved with output feedback.

Hindi and Boyd presented a set of tools to

perform local stability and performance analysis for linear systems with saturation [3], where the results were formulated in terms of linear matrix inequalities. Cao and Lin presented a stability analysis and design method for a class of nonlinear systems with saturation [4]. Particularly, T-S models with actuator saturation and norm-bounded uncertainty were used to describe the nonlinear system subject to actuator saturation, where a fuzzy scheduling controller design method was developed. In general, LMI approach, based on a convex optimization, may lead to less conservative information on stability regions, disturbance rejection, and  $L_2$ -gain than standard global stability and performance analysis. Recently, many applications via LMI have been attracted a lot of attentions, such as pole clustering and robustness. Chilali et. al. discussed the analysis techniques for robust pole placement in LMI regions [5]. For unstructured uncertainties, the Bounded Real Lemma characterization of quadratic stability has been generalized for pole clustering in arbitrary LMI regions. For parameter uncertainties, relying on scaling and multi-convexity techniques, two robust D-stability tests are derived [6]. A tractable LMI-based approach to the synthesis of output feedback controllers was proposed, in which the closed-loop poles can be robustly assigned in a prescribed LMI region. Furthermore, the robust pole placement techniques using  $H_\infty$  theory were also discussed. Fridman et. al. used  $H_\infty$  theory to analyze the system including time-delay and saturation [7]. Tseng and Chen developed the technique with neural network and LMI, where the  $H_2/H_\infty$  PID

tracking control design with regional pole constraints were discussed [8]. Ge et. al. also designed the robust PID controller via LQR-LMI approach [9].

Basically, referred to the existent results related to actuator saturation, the input signals are only considered in the linearly operational range for simplicity [4,10-11]. Hsu and Fong proposed a generalized sector condition for a linear system driven by actuators. A robust state feedback controller synthesis method was proposed to achieve the bounded control by linear matrix inequalities approach [12]. However, only the stability issue is addressed, and it is difficult to investigate additional performance, such as  $H_2$ .

In this paper, considering the limits of input for practical applications, stabilizing controller of input saturated system is addressed. First, the addressed saturation device is characterized in form of perturbation [13], thus the input signals are not necessarily in the linearly operational range. The controller is designed to make the poles of overall system to place in a certain stripe. It can be shown that the stability and the performance of system are satisfied with the performance requirements. The performances of interest include LMI pole regions assignment and the  $H_2$  performance index constraint. This paper is organized as follows. In Section 2, the formulation of input saturation and LMI-based regional stability are discussed. Sufficient conditions to ensure the pole placement with state feedback scheme are derived in Section 3. The  $H_2$  suboptimal control is also addressed. In Section 4, two numerical examples are used to illustrate the feasibility of the proposed works.

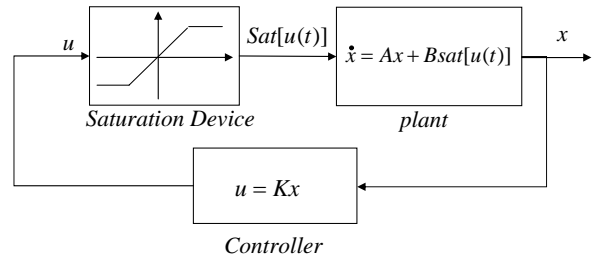


Fig. 1. The State feedback control structure with input saturation.

## II. PRELIMINARIES

### 2.1 Problem Statement

In Fig. 1, a continuous-time linear system with input saturation is given

$$\dot{x}(t) = A \cdot x(t) + B \cdot \text{sat}[u(t)] \quad (1)$$

where  $x \in R^{n \times 1}$  is state variable,  $A \in R^{n \times n}$ ,  $B \in R^{n \times l}$ ,  $u \in R^{l \times 1}$ , and the saturated input  $\text{sat}[u(t)] \in R^{l \times 1}$ . The matrix pair  $(A, B)$  is assumed to be controllable. Fig. 2 indicates the characteristic of the constrained input, which is represented in the following

$$\text{sat}[u(t)] = \begin{cases} u_{jH}, & 0 < u_{jH} \leq u(t) \\ u(t), & u_{jL} \leq u(t) \leq u_{jH} \\ u_{jL}, & u(t) \leq u_{jL} < 0 \end{cases} \quad (2)$$

where  $u_{jH}$  and  $u_{jL}$  are the bounds of linear operation range of  $u(t)$ .

Without loss of generality, it is supposed that  $u_{jL} = -u_{jH}$ . It is also noted that there is a line through the origin point with slope  $m = a_j$ , where  $u_{jH}/a_j$  and  $u_{jL}/a_j$  are the maximum and

minimum allowable inputs of saturation device, respectively. In the allowable range of input,  $u(t) \in [u_{jL}/a_j, u_{jH}/a_j]$ , it can be seen that

$$\text{sat}[u_j(t)] - \frac{1}{2}(1+a_j)u_j(t) = \Delta S_j \cdot u_j(t) \quad (3)$$

where

$$-\frac{1}{2}(1-a_j) \leq \Delta S_j \leq \frac{1}{2}(1-a_j), \quad j=1,2,\dots,l \quad (4)$$

Define

$$W = \begin{bmatrix} W_1 & & & \\ & W_2 & & \\ & & \ddots & \\ & & & W_l \end{bmatrix}$$

in which

$$W_j = \frac{1}{2}(1-a_j), \quad j=1,2,\dots,l$$

Thus, the magnitude of  $\Delta S_j$  satisfies that

$$|\Delta S_j| \leq W_j, \quad j=1,2,\dots,l \quad (5)$$

In matrix form, the saturation input can be described as follows

$$\text{sat}[u(t)] = V \cdot u(t) + \Delta S \cdot u(t) \quad (6)$$

where

$$\text{sat}[u(t)] = \begin{bmatrix} \text{sat}[u_1(t)] \\ \text{sat}[u_2(t)] \\ \vdots \\ \text{sat}[u_l(t)] \end{bmatrix} \quad V = \begin{bmatrix} \frac{1+a_1}{2} & & & \\ & \frac{1+a_2}{2} & & \\ & & \ddots & \\ & & & \frac{1+a_l}{2} \end{bmatrix}$$

$$\Delta S = \begin{bmatrix} \Delta S_1 & & & \\ & \Delta S_2 & & \\ & & \ddots & \\ & & & \Delta S_l \end{bmatrix}$$

It is clear that  $\Delta S, V$ , and  $W$  are symmetric. Also, it can be seen that  $\Delta S - W \leq 0$  and  $\Delta S^T \Delta S - W^T W \leq 0$ . The purpose of this paper is to find a stabilizing state-feedback controller  $u(t) = Kx(t)$  such that certain regional placement performances of system (1) are satisfied.

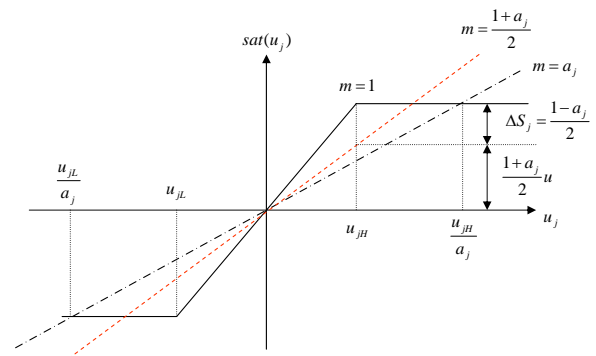


Fig. 2. Input-output characteristics of the saturation device.

## 2.2 LMI Regions

An LMI region  $D$  of the complex plane can be represented as [5,6]

$$D = \{z \in \mathbb{C} : L + zM + \bar{z}M^T\} \quad (7)$$

where  $L \in \mathbb{R}$ ,  $M \in \mathbb{R}$ ,  $L = L^T$ . The associated characteristic function of  $D$  is defined by

$$f_D = L + zM + \bar{z}M^T \quad (8)$$

For instance, a subregion in the open left half plane,  $\text{Re}(z) < -\alpha$ , can be modeled as a LMI region, where the associated characteristic equation is

$$f_D(z) = z + \bar{z} + 2\alpha < 0 \quad (9)$$

Considering the unforced system of (1),

$$\dot{x}(t) = Ax(t)$$

the system matrix  $A$  is stable corresponding to  $\text{Re}(z) < -\alpha$ , if and only if there exists a symmetric matrix  $P > 0$  such that the following linear matrix inequality is hold [5,14].

$$PA + A^T P + 2\alpha P < 0 \quad (10)$$

Choose  $V(x)$  as a Lyapunov function candidate

$$V(x(t)) = x^T(t)Px(t) \quad (11)$$

Taking the derivative of  $V(x)$ , from (10), we have

$$\dot{V}(x(t)) = \dot{x}^T(t)Px(t) + x^T(t)P\dot{x}(t) < -2\alpha V(x(t)) \quad (12)$$

Equivalently, it can be obtain that  $V(x(t)) < e^{-2\alpha t}V(x(0))$  [11], that is

$$x^T(t)Px(t) < e^{-2\alpha t}x^T(0)Px(0) \quad (13)$$

**Remark 1** We can use the MATLAB LMI

toolbox [14] to solve the inequality problem of (10) about regional pole placement which infects the system performances.

**Remark 2** Setting  $Y = P^{-1}$ , the decay rate constraint of state trajectory can be also represented as

$$AY + YA^T < -2\alpha Y \quad (14)$$

### 2.3 Input Limits

In practice, the control inputs are limited with a specified bound. A typical norm-bounded input is  $\|u(t)\| \leq \mu, \mu > 0$ ,  $u(t) = Kx(t)$ , and the associated LMIs are represented as [15]

$$\begin{bmatrix} 1 & x^T(0) \\ x(0) & Y \end{bmatrix} \geq 0 \quad (15)$$

$$\begin{bmatrix} Y & Z^T \\ Z & \mu^2 I \end{bmatrix} \geq 0 \quad (16)$$

where  $Z = KY$ ,  $Y = P^{-1}$  is symmetric and positive definite and  $Z$  satisfies the stabilizability conditions. Thus, if the initial condition of state is given, we can find an upper norm bound of the control input.

## III. REGIONAL STABILITY AND $H_2$ CONTROL

From (1), (6), the feedback control scheme,  $u(t) = Kx(t)$ , can be described as follows

$$\dot{x}(t) = (A + BVK + B\Delta SK) \cdot x(t) \cong A_K x(t) \quad (17)$$

The pole region considered in this paper is shown as Fig. 3(a). It can be seen that the region of Fig. 3(a) is the intersection of two half planes, Fig. 3(b),(c).

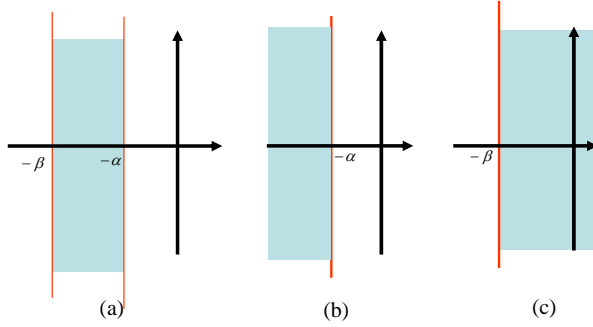


Fig. 3. The LMI Pole Regions

### 3.1 Half-Plane Pole Regions

The following derivations are based on the assumption that there exists a  $K$  such that

$$[B^T P - \Delta SK]^T [B^T P - \Delta SK] \geq 0 \quad (18)$$

and

$$[B^T P + \Delta SK]^T [B^T P + \Delta SK] \geq 0 \quad (19)$$

Equivalently, we have

$$\begin{aligned} PBB^T P + K^T \Delta S^T \Delta SK \\ - PB \Delta SK - K^T \Delta S^T B^T P \geq 0 \end{aligned} \quad (20)$$

and

$$\begin{aligned} PBB^T P + K^T \Delta S^T \Delta SK \\ + PB \Delta SK + K^T \Delta S^T B^T P \geq 0 \end{aligned} \quad (21)$$

From (10), the eigenvalues of (17) are in Fig. 3(b), if

$$PA_K + A_K^T P + 2\alpha P < 0 \quad (22)$$

Substituting  $A_K = A + BVK + B\Delta SK$  into (22), it yields

$$\begin{aligned} PA + A^T P + PB VK + K^T V^T B^T P \\ + PB \Delta SK + K^T \Delta S^T B^T P + 2\alpha P < 0 \end{aligned} \quad (23)$$

From (20), the sufficient condition for ensuring the eigenvalues of the closed-loop system are in the region of Fig. 3(b) is

$$\begin{aligned} PA + A^T P + PB VK + K^T V^T B^T P \\ + PBB^T P + K^T \Delta S^T \Delta SK + 2\alpha P < 0 \end{aligned} \quad (24)$$

Using the fact that  $\Delta S^T \Delta S \leq W^T W$ , a sufficient condition of (24) is

$$\begin{aligned} PA + A^T P + PB VK + K^T V^T B^T P \\ + PBB^T P + K^T W^T W K + 2\alpha P < 0 \end{aligned} \quad (25)$$

Substituting  $Z = KY$ ,  $Y = P^{-1}$  into (25), we have

$$\begin{aligned} AY + YA^T + BVZ + Z^T V^T B^T \\ + BB^T + Z^T W^T W Z + 2\alpha Y < 0 \end{aligned} \quad (26)$$

By Schur Complement [11], (26) can be reformulated as

$$\begin{bmatrix} \left( \begin{array}{c} AY + YA^T + BVZ \\ + Z^T V^T B^T + BB^T + 2\alpha Y \end{array} \right) & Z^T W^T \\ WZ & -I \end{bmatrix} < 0 \quad (27)$$

The discussion of deriving pole-assignment conditions associated with Fig. 3(c) is based on a certain symmetric property of eigenvalues.

Consider the fact that  $\text{Re}[\lambda_i(-A_k)] < \beta$  implies that  $\text{Re}[\lambda_i(A_k)] > -\beta$ . Thus, corresponding to the region of Fig. 3(c), the pole placement condition of (17) is

$$P(-A_k) + (-A_k)^T P - 2\beta P < 0 \quad (28)$$

or

$$PA_k + A_k^T P + 2\beta P > 0 \quad (29)$$

Substituting  $A_k = A + BVK + B\Delta SK$  into (29), it yields

$$PA + A^T P + PBVK + K^T V^T B^T P - PB\Delta SK - K^T \Delta S^T B^T P + 2\beta P > 0 \quad (30)$$

From (21) using the fact that  $-\Delta S^T \Delta S \geq -W^T W$ , a sufficient condition of (30) is

$$PA + A^T P + PBVK + K^T V^T B^T P - PBB^T P - K^T W^T W K + 2\beta P > 0 \quad (31)$$

Equivalently, taking  $Z = KY$ ,  $Y = P^{-1}$ , it can be obtained that

$$AY + YA^T + BVZ + Z^T V^T B^T - BB^T - Z^T W^T W Z + 2\beta Y > 0 \quad (32)$$

By Schur Complement, an equivalent LMI formulation of (32) is

$$\begin{bmatrix} \left( \begin{array}{c} AY + YA^T + BVZ \\ + Z^T V^T B^T - BB^T + 2\beta Y \end{array} \right) & Z^T W^T \\ WZ & -I \end{bmatrix} > 0 \quad (33)$$

which ensures that the eigenvalues of (17) are in Fig. 3(c).

### 3.2 $H_2$ Control

A standard  $H_2$  performance index is defined as follows [8]

$$J = \int_0^t (x^T Q x + u^T R u) dt \quad (34)$$

where  $Q > 0$ ,  $R > 0$ . Therefore, a suboptimal approach is taken by minimizing the upper bound of the performance index. Observe that

$$\begin{aligned} J &= \int_0^{t_f} (x^T Q x + u^T R u) dt \\ &= x^T(0) P x(0) - x^T(t_f) P x(t_f) \\ &\quad + \int_0^{t_f} [x^T Q x + u^T R u + \frac{d}{dt}(x^T P x)] dt \\ &\leq x^T(0) P x(0) - x^T(t_f) P x(t_f) \\ &\quad + \int_0^{t_f} [x^T Q x + u^T R u + \dot{x}^T P x + x^T P \dot{x}] dt \end{aligned} \quad (35)$$

Considering the state dynamics (17), we have

$$\begin{aligned} J &\leq x^T(0) P x(0) - x^T(t_f) P x(t_f) \\ &\quad + \int_0^{t_f} [x^T \hat{C}^T Q \hat{C} x + u^T R u \\ &\quad + (Ax + BVKx + B\Delta SK)^T P x \\ &\quad + x^T P (Ax + BVKx + B\Delta SK)] dt \\ &= x^T(0) P x(0) - x^T(t_f) P x(t_f) \\ &\quad + \int_0^{t_f} \{x^T [\hat{C}^T Q \hat{C} + K^T R K \\ &\quad + (A + BVK + B\Delta SK)^T P x \\ &\quad + P (Ax + BVKx + B\Delta SK)] x\} dt \end{aligned} \quad (36)$$

It is clear that if the following inequality holds

$$\begin{aligned} & Q + K^T R K + A^T P + K^T V^T B^T P \\ & + K^T \Delta S^T B^T P + P A + P B V K + P B \Delta S K < 0 \end{aligned} \quad (37)$$

the cost  $J$  satisfies that

$$J \leq x^T(0) P x(0) \quad (38)$$

Taking  $Z = KY$ ,  $Y = P^{-1}$ , and  $\Delta S^T \Delta S \leq W^T W$ , a sufficient condition of (37) is

$$\begin{aligned} & Y Q Y + Z^T R Z + Y A^T + Z^T V^T B^T \\ & + A Y + B V Z + B B^T + Z^T W^T W Z < 0 \end{aligned} \quad (39)$$

By Schur Complements, (39) becomes

$$\begin{bmatrix} \left( \begin{array}{c} Y A^T + A Y + Z^T V^T B^T \\ + B V Z + B B^T \end{array} \right) & Z & Y \hat{C}^T & Z^T W^T \\ Z & -R^{-1} & 0 & 0 \\ \hat{C} Y & 0 & -Q^{-1} & 0 \\ W Z & 0 & 0 & -I \end{bmatrix} < 0 \quad (40)$$

Suppose  $\delta > 0$  and

$$J \leq x^T(0) P x(0) < \delta \quad (41)$$

Equivalently, with the Schur Complement, (41) implies that

$$\begin{bmatrix} \delta & x^T(0) \\ x(0) & P^{-1} \end{bmatrix} > 0 \quad (42)$$

or

$$\begin{bmatrix} \delta & x^T(0) \\ x(0) & Y \end{bmatrix} > 0 \quad (43)$$

Therefore, the suboptimal  $H_2$  control problem can be solved by LMI formulation.

**Remark 3** Given  $\alpha$ ,  $\beta$ ,  $\delta$ , for a input saturated system (1), a state feedback controller  $u(t) = Kx(t)$  can be obtained such that the stripe stability and suboptimal  $H_2$  performance are satisfied, if LMIs of (27), (33), (40), and (43) are solved.

## IV. Numerical Examples

### 4.1 MIMO Case

A continuous time system with input constraint is given as follows [13]

$$\begin{bmatrix} \dot{x}_1(t) \\ \dot{x}_2(t) \end{bmatrix} = \begin{bmatrix} -4 & 2 \\ -3 & 1 \end{bmatrix} \begin{bmatrix} x_1(t) \\ x_2(t) \end{bmatrix} + \begin{bmatrix} 1 & 0.1 \\ 0.2 & 1 \end{bmatrix} \begin{bmatrix} \text{sat}[u_1(t)] \\ \text{sat}[u_2(t)] \end{bmatrix} \quad (44)$$

where  $x(t_0) = [0.2 \ 0.1]^T$ . Referred to Fig. 2, let  $a_1 = 0.4$ ,  $a_2 = 0.3$ ,  $u_{1H} = 0.4$ ,  $u_{2H} = 0.3$ . Also, it can be obtained that

$$V = \begin{bmatrix} 0.7 & 0 \\ 0 & 0.65 \end{bmatrix}, \quad W = \begin{bmatrix} 0.3 & 0 \\ 0 & 0.35 \end{bmatrix}$$

where the pair  $(A, B)$  is controllable. Let the prespecified stripe region be described by  $\alpha = 1$  and  $\beta = 4$ . The  $H_2$  performance index is set by  $\delta = 0.05$ . The constraints of this case include a LMI pole region and maximum input signal  $u_{\max} = u_{jH} / a_j = 1$ ,  $j = 1, 2$ . The saturation value of each input channel is  $u_{1H} = 0.4$ ,  $u_{2H} = 0.3$ , respectively. From Eqs. (15), (16), (27), (33), (40), and (43) by using MATLAB LMI Toolbox, we obtain the state feedback gain



$$K = \begin{bmatrix} -0.6060 & 0.4558 \\ 0.5588 & -0.6198 \end{bmatrix}$$

provided with a positive definite  $P$ ,

$$P = \begin{bmatrix} 0.7615 & -0.6641 \\ -0.6641 & 0.6376 \end{bmatrix}$$

The time responses of system states and input signals are shown in Figs. 4-5.

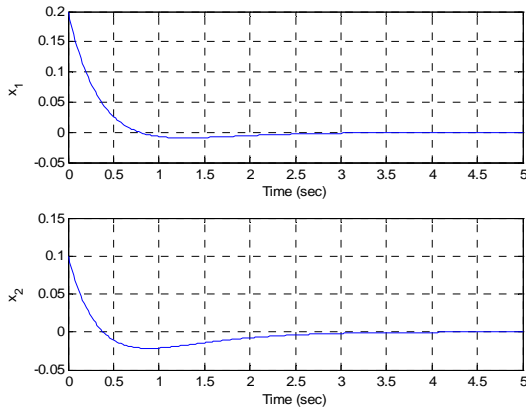


Fig. 4. The time responses of states  $x_1$  and  $x_2$

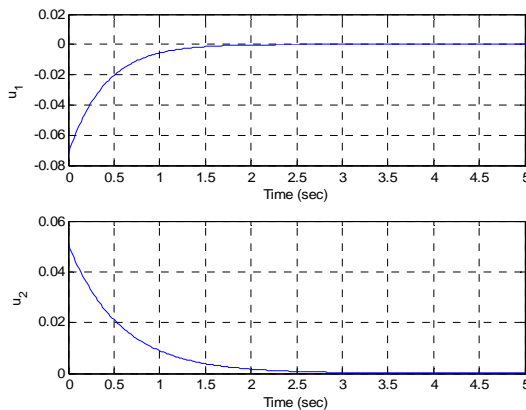


Fig. 5. The time responses of states  $u_1$  and  $u_2$

The trajectory of energy function  $V(x)$  is

between  $V(0)e^{-2t}$  and  $V(0)e^{-8t}$  as desired, shown in Fig. 6. The time response of cost  $J$  is shown in Fig. 7, where its steady state value is 0.0008123 which is smaller than  $\delta = 0.05$ . In fact, the histories of input signals stay in the constrained region as required.

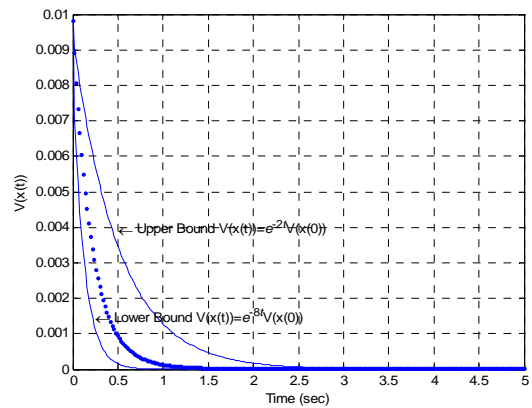


Fig. 6. The decay rate bound and time response of energy function  $V(x)$

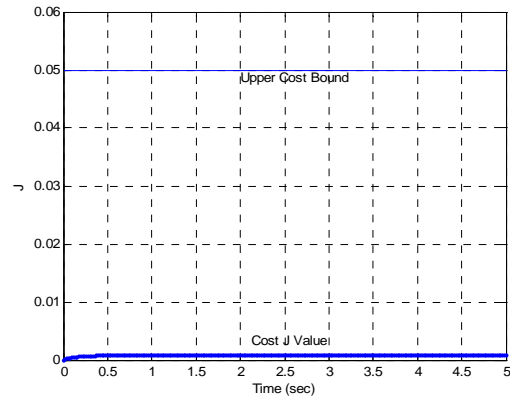


Fig. 7. The Cost bound and time response of Cost function  $J$

## 4.2 Inverted Pendulum on a Cart

Consider the problem of a balance inverted pendulum on a cart [4,15], shown by Fig. 8. The dynamics of the addressed pendulum are

Fig. 8. Inverted Pendulum on a Cart.

$$\dot{x}_1 = x_2 \quad (45)$$

$$\dot{x}_2 = \frac{g \sin(x_1) - \frac{amlx_2^2 \sin(2x_1)}{2} - \gamma a \cos(x_1) \text{sat}[u(t)]}{\frac{4}{3}l - aml \cos^2(x_1)} \quad (46)$$

$$a = \frac{1}{M + m} \quad (47)$$

where  $x_1$  is the angle of the pendulum in radians from the vertical,  $x_2$  is the angular speed,  $g = 9.8 \text{ m/s}^2$  is the gravity constant,  $M$  is the mass of the cart,  $m$  is the mass of the pendulum,  $l$  is the half length of the pendulum, and  $u$  is the force applied to the cart.

Without loss of generality, it is chosen that  $m = 2 \text{ Kg}$ ,  $M = 8 \text{ Kg}$ ,  $l = 5 \text{ m}$ ,  $\gamma = 1000$ . The actuator is subject to saturation and the saturation level is  $u_{\max} = 4$ . The maximum input signal of the saturation device is  $\mu = 8$ . Linearizing the nonlinear dynamics (45)-(47) about the equilibrium point,  $x_1(0) = x_2(0) = 0$ , it yields the following linearized model

$$\begin{bmatrix} \dot{x}_1(t) \\ \dot{x}_2(t) \end{bmatrix} = \begin{bmatrix} 0 & 1 \\ \frac{g}{\frac{4}{3}l - aml} & 0 \end{bmatrix} \begin{bmatrix} x_1(t) \\ x_2(t) \end{bmatrix} + \begin{bmatrix} 0 \\ \frac{-\gamma a}{\frac{4}{3}l - aml} \end{bmatrix} \text{sat}[u(t)] \quad (48)$$

Let the prespecified stripe subregion be described by  $\alpha = 5$ ,  $\beta = 35$ . The saturation value of input is  $u_H = 4$ . We can calculate that  $a_1 = 0.5$ ,  $V = 0.75$ ,  $W = 0.25$ . Without loss of generality, initial condition is  $x_1(0) = 60^\circ$ ,  $x_2(0) = 0^\circ$ . By using MATLAB LMI Toolbox, a stabilizing state feedback,  $u(t) = Kx(t)$ , is obtained,

$$K = [1.9649 \quad 0.2087]$$

provided with a positive definite  $P$

$$P = \begin{bmatrix} 0.1308 & 0.0046 \\ 0.0046 & 0.0007 \end{bmatrix}$$

It can be checked that the eigenvalues of the linearized system are negative,  $-13.8646 \pm 5.8029i$ . Thus, by Lyapunov indirect method [16], the original system around the equilibrium point is asymptotically stable. The  $H_2$  performance index value is given as  $\delta = 0.7$ . The closed-loop system with five different initial conditions,  $[x_1(0) \quad x_2(0)] = [20^\circ \quad 0]$ ,  $[40^\circ \quad 0]$ ,  $[60^\circ \quad 0]$ , are investigated. The time responses of states and input force are shown in Figs. 9-11. The trajectories of time responses of energy function  $V(x)$  are indeed between  $V(x)e^{-10t}$  and  $V(x)e^{-70t}$ , shown in Figs 12-14. The time response of cost  $J$  is shown as Fig. 15. In our design, the maximum  $H_2$  performance index value is 0.0905 that is smaller than 0.7 as request. Simulation results indicate that the closed-loop system is regional stable corresponding to a designated stripe.

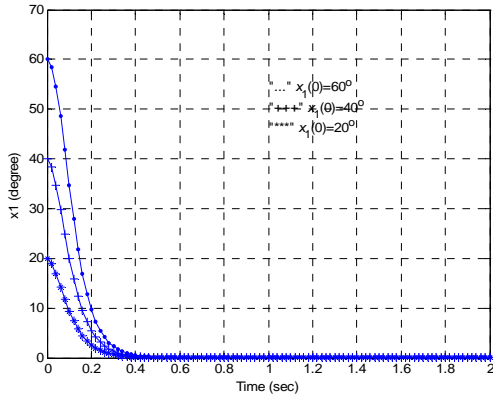


Fig. 9. Angle degrees of Inverted Pendulum on a cart with all initial conditions

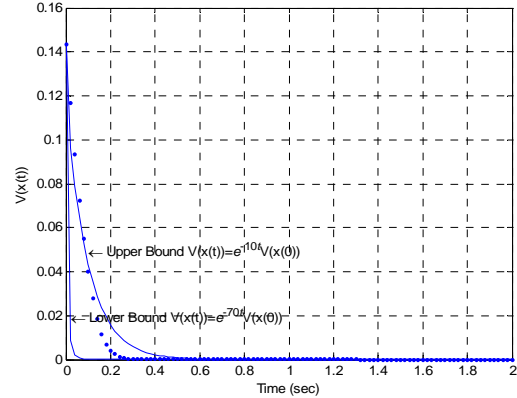


Fig. 12. The decay rate bound and time response of energy function  $V(x)$  ( $x_1(0) = 60^0$ )

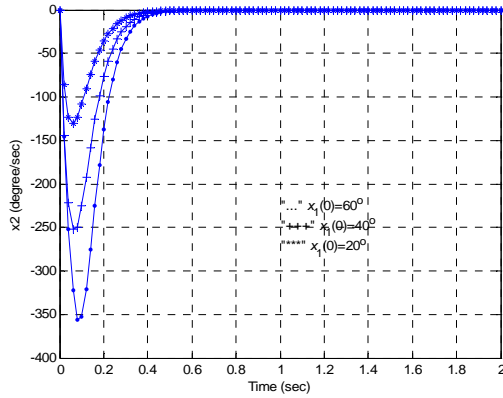


Fig. 10. Angle speed of Inverted Pendulum on a cart with all initial conditions

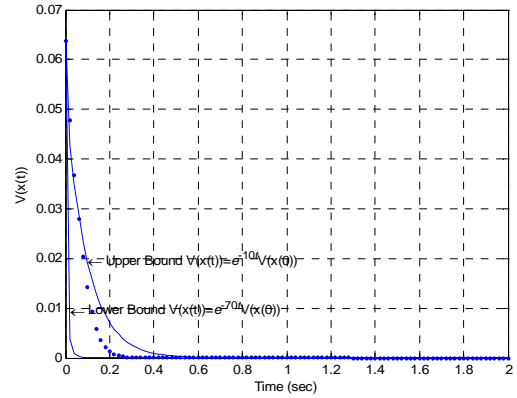


Fig. 13. The decay rate bound and time response of energy function  $V(x)$  ( $x_1(0) = 40^0$ )

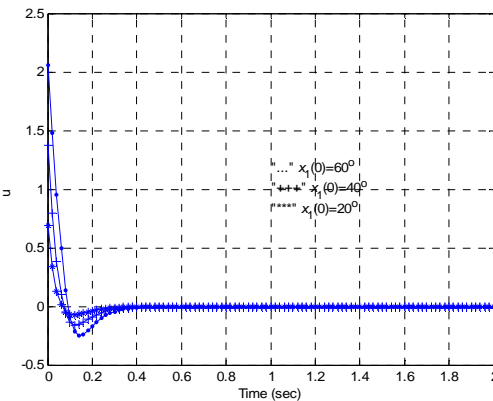


Fig. 11. Control input of Inverted Pendulum on a cart with all initial conditions

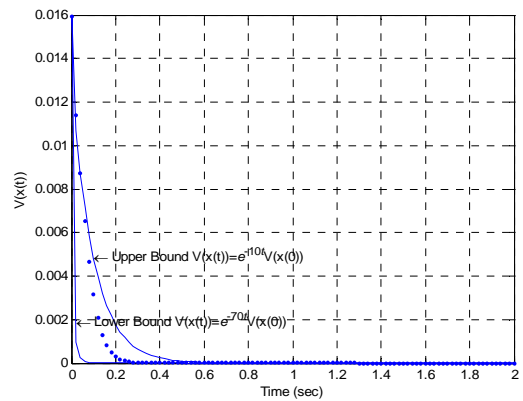


Fig. 14. The decay rate bound and time response of energy function  $V(x)$  ( $x_1(0) = 20^0$ )

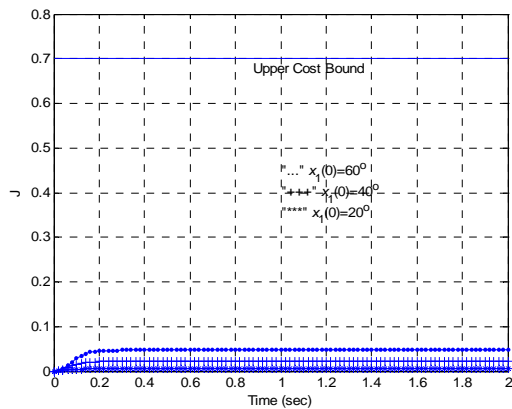


Fig. 15. The Cost bound and time response of Cost function  $J$  with all initial conditions

## V. CONCLUSION

In this paper, a multiobjective controller design with input saturation is investigated. The performances of interest include regional stability, input constraint, and  $H_2$  performance. Sufficient conditions are derived to ensure the stability of constrained input system, where the LMI formulations are derived. Two numerical examples are provided to investigate the feasibility of proposed works. Simulation results illustrate that the required multiobjective performances are achieved.

## REFERENCE

- [1] Saberi, A. and Stoorvogel, A. A. (eds), "Special issue on control problems with constraints," *International Journal of Robust and Nonlinear Control*, Vol. 9, pp.583-734, 1999.
- [2] Saberi, A., Lin, Z., and Teel, A. R., "Control of linear systems with saturating actuators," *IEEE Trans. on Automatic Control*, Vol. 41, No. 3, pp.368-378, 1996.
- [3] Hindi, H. and Boyd, S., "Analysis of linear systems with saturating using convex optimization," in *Proc. of the 37th CDC*, pp.903-908, Florida, USA, Dec. 1998.
- [4] Cao, Y. Y. and Lin, Z., "Roust stability analysis and fuzzy-scheduling control for nonlinear system subject to actuator saturation," *IEEE Trans. on Fuzzy Systems*, Vol. 11, No. 1, pp.57-67, 2003.
- [5] Chilali, M., Gahinet, P., and Apkarian, P., "Robust pole placement in LMI regions," *IEEE Trans. on Automatic Control*, Vol. 44, No. 12, pp.2257-2270, 1999.
- [6] Chilali, M. and Gahinet, P., " $H_\infty$  design with pole placement constraints: a LMI approach," *IEEE Trans. on Automatic Control*, Vol. 41, No. 3, pp.358-367, 1996.
- [7] Fridman, E., Pila, A., and Shaked, U., "Regional stabilization and control of time-delay systems with saturating actuators," *Int. J. of Robust Nonlinear Control*, Vol. 13, pp.885-907, 2003.
- [8] Tseng, C.S. and Chen, B.S., "Multiobjective PID control design in uncertain robotic systems using neural network elimination scheme," *IEEE Trans. on Systems, Man, and Cybernetics-Part A: Systems and Humans*, Vol. 31, No. 6, pp.632-644, 2001.
- [9] Ge, M., Chiu, M.S., and Wang, Q.G., "Robust PID controller design via LMI approach," *J. of Process Control*, Vol. 12, pp.3-13, 2002.
- [10] Astrom, K.J. and Hagglund, T., PID

Controllers, 2nd Edition, Research Triangle Park, NC, ISA, 1995.

- [11] Boyd, S., Ghaoui, L. El, Feron, E., and Balakrishnan, V., Linear Matrix Inequalities in System and Control Theory, Philadelphia, U.S.A., PA: SIAM, 1994.
- [12] Hsu, C. C. and Fong, I. K., "Robust state feedback control through actuators with generalized sector nonlinearities and saturation," *Asian Journal of Control*, Vol. 5, No. 3, pp.382-389, 2003.
- [13] Chang, Y.-H. and Chang, J.-C., "Robust wedge-stability analysis and design of continuous constrained systems with stability radii," *Internal Journal of Systems Science*, Vol. 31, No. 9, pp.1067-1075, 2000.
- [14] Gahinet, P., Nemirovski, A., Laub, A. J., and Chilali, M., LMI Control Toolbox, U.S.A., The MathWorks Inc., 1995.
- [15] Tanaka, K. and Wang, H. O., Fuzzy Control Systems Design and Analysis, U.S.A., Wiley- Interscience, 2001.
- [16] Khalil, H.K., Nonlinear System, U.S.A., Prentice-Hall Inc., 2002.